Pflugers Arch - Eur J Physiol (2017) 469:1287–1299
DOI 10.1007/s00424-017-1989-8

Na^+/Ca^{2+} exchangers and Orai channels jointly refill endoplasmic reticulum (ER) Ca^{2+} via ER nanojunctions in vascular endothelial cells

Cristiana M. L. Di Giuro[1] · Niroj Shrestha[1] · Roland Malli[2] · Klaus Groschner[1] · Cornelis van Breemen[3] · Nicola Fameli[1]

Received: 31 March 2017 / Revised: 20 April 2017 / Accepted: 24 April 2017 / Published online: 11 May 2017

Abstract We investigated the role of Na^+/Ca^{2+} exchange (NCX) in the refilling of endoplasmic reticulum (ER) Ca^{2+} in vascular endothelial cells under various conditions of cell stimulation and plasma membrane (PM) polarization. Better understanding of the mechanisms behind basic ER Ca^{2+} content regulation is important, since current hypotheses on the possible ultimate causes of ER stress point to deterioration of the Ca^{2+} transport mechanism to/from ER itself. We measured $[Ca^{2+}]_i$ temporal changes by Fura-2 fluorescence under experimental protocols that inhibit a host of transporters (NCX, Orai, non-selective transient receptor potential canonical (TRPC) channels, sarco/endoplasmic reticulum Ca^{2+} ATPase (SERCA), Na^+/K^+ ATPase (NKA)) involved in the Ca^{2+} communication between the extracellular space and the ER. Following histamine-stimulated ER Ca^{2+} release, blockade of NCX Ca^{2+}-influx mode (by 10 μM KB-R7943) diminished the ER refilling capacity by about 40%, while in Orai1 dominant negative-transfected cells NCX blockade attenuated ER refilling by about 60%. Conversely, inhibiting the ouabain sensitive NKA (10 nM ouabain), which may be localized in PM-ER junctions, increased the ER Ca^{2+} releasable fraction by about 20%, thereby supporting the hypothesis that this process of privileged ER refilling is junction-mediated. Junctions were observed in the cell ultrastructure and their main parameters of membrane separation and linear extension were (9.6 ± 3.8) nm and (128 ± 63) nm, respectively. Our findings point to a process of privileged refilling of the ER, in which NCX and store-operated Ca^{2+} entry via the stromal interaction molecule (STIM)-Orai system are the sole protagonists. These results shed light on the molecular machinery involved in the function of a previously hypothesized subplasmalemmal Ca^{2+} control unit during ER refilling with extracellular Ca^{2+}.

Keywords Endothelium · Calcium signals · ER junctions · NCX · Orai1 · EA.hy926

This article is part of the Topical Collection on *Ion channels, receptors and transporters*

Electronic supplementary material The online version of this article (doi:10.1007/s00424-017-1989-8) contains supplementary material, which is available to authorized users.

✉ Nicola Fameli
nicola.fameli@medunigraz.at; nicola.fameli@ubc.ca

[1] Institute of Biophysics, Medical University of Graz, Graz, Austria

[2] Institute of Molecular Biology & Biochemistry, Medical University of Graz, Graz, Austria

[3] BC Children's Hospital Research Institute, Department of Anaesthesiology, Pharmacology & Therapeutics, University of British Columbia, Vancouver, British Columbia, Canada

Introduction

Activation of non-excitable cells, like endothelial cells (EC), by receptor agonists typically provokes an increase in inositol 1,4,5-trisphosphate (IP_3) and consequent endoplasmic reticulum (ER) Ca^{2+} release via IP_3 receptors (IP_3R). The subsequent $[Ca^{2+}]_i$ elevation is a preamble underpinning basic EC function like nitric oxide (NO) synthesis by the endothelial NO synthase and endothelin-1 production [19, 32, 38, 47]. While store-operated Ca^{2+} entry (SOCE) is generally considered the main (if not sole) mechanism responsible for cytosolic Ca^{2+} resetting and ER Ca^{2+} refilling following stimulation [2, 30], and evidence exists for

a role of mitochondria in ER Ca^{2+} regulation [30, 31], there is reason to consider that Na^+/Ca^{2+} exchange (NCX) may also play an important role in this process. In fact, the Na^+/Ca^{2+} exchanger, whose existence in EC has long been reported [7] (more specifically we will refer herein to the NCX1 isoform—the most abundantly expressed in EC [45, 48]), has been shown to play an important role in Ca^{2+} extrusion from these cells once the stimulus is removed in low external Ca^{2+} conditions as well as during acetylcholine and histamine stimulation under physiological conditions [5, 29, 56]. In addition to its Ca^{2+} extrusion operation, the NCX Ca^{2+} influx mode has been observed to perform a fundamental function in Ca^{2+} refilling of sarco/endoplasmic reticulum (S/ER) in vascular smooth muscle cells [27] and it has also been suggested that it plays a role in activating angiogenesis function in EC [1]. Therefore, in this article, we report on our in-depth studies of the role of NCX for ER Ca^{2+} refilling in human umbilical vein derived EC (EA.hy926 [10]).

An important feature of NCX-mediated S/ER Ca^{2+} refilling in earlier observations in vascular smooth muscle cells, as well as Ca^{2+} removal in EC, is that it appears to occur via plasma membrane (PM)-S/ER nanojunctions [14, 26, 27, 56]. Generally speaking, these are intracellular regions comprising portions of the PM and of the S/ER membrane separated by 10–30 nm and extending roughly parallel to each other for several hundred nanometers, the intervening cytosolic space and the local ion transport machinery (channels, pumps, exchangers). The role of nanojunctions in assisting cell signaling has been recognized as pivotal in several systems [37, 54]. Interestingly, there is also strong evidence that the subplasmalemmal region of EC is involved in a crucial way in Ca^{2+} extrusion mechanisms, in a manner that shunts the bulk cytoplasm; indeed, this has led to the hypothesis of a "subplasmalemmal Ca^{2+} control unit (SCCU)" akin to the "superficial buffer barrier" of vascular smooth muscle cells [16, 40, 53]. Hence, in the present study, we also addressed the important hypothesis that NCX-mediated Ca^{2+} transport in EC occurs via PM-ER junctions.

To provide the right setting of our findings, it is useful to recall the current knowledge of the machinery purportedly responsible for Ca^{2+} handling in EC. Due to the apparent lack of a functional role for voltage-gated cation channels in EC [18, 50], Ca^{2+} entry in these cells depends upon receptor operated channels, predominantly channels of the non-selective transient receptor potential canonical (TRPC) family, and the highly Ca^{2+} selective Orai1 store operated channels, the latter only operative when clustered in PM-ER junctions, upon depletion of the ER Ca^{2+} [34]. Furthermore, Ca^{2+} can be pumped into the ER by the S/ER Ca^{2+} ATPases (SERCA), and released from the ER via the IP_3R and ryanodine receptor channels. However, while the latter have been observed by immunofluorescence [28] and implicated in the ER Ca^{2+} release in the subplasmalemmal region of EC [5, 16, 29, 40, 56], they do not appear to be expressed in the EA.hy926 cell line [23].

Due to the reported variability of the EC's membrane potential, V_m, (see [41] and references therein) and the necessity to operate with a stable driving force of the NCX, we opted to work under conditions of membrane depolarization by using a superfusing solution with 70 mM $[K^+]$ (with ≈70 mM $[Na^+]$ for osmotic balance). This "driving force clamp" method has been employed before [24] and in our experiments also serves the purpose of highlighting the NCX-mediated Ca^{2+} influx in relation to that of TRPC and Orai1.

In the present study, we report Fura-2-based $[Ca^{2+}]_i$ measurements under a host of conditions aimed at elucidating the role of NCX in the refilling of ER Ca^{2+} via PM-ER nanojunctions. We also provide novel ultrastructural evidence of PM-ER junctions and quantitative characterization thereof in EC.

Materials and methods

Materials

Cell culture chemicals were obtained from Thermo Fisher Scientific; histamine, amphotericin B (AmB), KCl, $MgCl_2$, $CaCl_2$, glucose, HEPES, EGTA, 2-aminoethoxydiphenyl borate (2-APB), and ouabain from Sigma-Aldrich, NaCl from Carl Roth. KB-R7943 was purchased from Sigma-Aldrich and Abcam. We used Fura-2 AM products by both Sigma-Aldrich and Thermo Fisher Scientific.

Cell culture and transfection

Experiments were performed with the human umbilical vein endothelium derived cell line, EA.hy926 [10]. Cells were cultured in Dulbecco's modified Eagle medium (DMEM) containing 10% fetal bovine serum, 100 U/mL penicillin, 100 µg/mL streptomycin, and HAT (50 µM hypoxanthin, 0.2 µM aminopterin, 0.8 µM thymidine, and 1.25 µg/mL AmB) and were maintained in an incubator at 37 °C in 5% CO_2 atmosphere. The cells were used at passages between 30 and 80 and were plated on 6 mm × 6 mm square cover slips for transfection and experiments at a confluence of 50–80%.

For the experiments in absence of functional Orai1, cells were transiently transfected with 1.5 µg E106 dominant-negative Orai1 ($Orai1^{dn}$) cDNA using TransFast™ Transfection Reagent (Promega) in DMEM following manufacturer's instructions. After 4–6-h incubation, the transfection

mixture was replaced by normal culture medium. Ca^{2+} measurements were performed 24–48 h after transfection. The transfection efficiency was between 15 and 25% and was determined by inspection of fluorescence images. YFP-tagged $Orai1^{dn}$ were localized to the PM. To ensure that the transfection process did not appreciably affect the Ca^{2+} signals, we performed control experiments with cells sham-transfected with cytosolic YFP and compared their Fura-2 fluorescence to that of non-transfected cells. The two sets did not significantly differ (see section S1 in the online supplement), which gives us confidence that the non-transfected cells are a proper control for these experiments.

Solutions

The normal experimental buffer (EB) was composed of (in mM) 138 NaCl, 5 KCl, 2 $CaCl_2$, 1 $MgCl_2$, 10 glucose, and 10 HEPES, pH adjusted to 7.4 with NaOH.

The 70 mM $[K^+]_o$ EB was composed of (in mM) 73 NaCl, 70 KCl, 2 $CaCl_2$, 1 $MgCl_2$, 10 glucose, and 10 HEPES, pH adjusted to 7.4 with KOH. The Ca^{2+}-free EB contained 0.1 mM EGTA instead of $CaCl_2$.

The loading buffer solution (LB) contained (in mM unless otherwise indicated) 135 NaCl, 5 KCl, 2 $CaCl_2$, 1 $MgCl_2$, 10 HEPES, 2.6 $NaHCO_3$, 0.44 KH_2PO_4, 10 glucose with 0.1% vitamins and 0.2% essential amino acids, 1% penicillin/streptomycin, and 1.25 µg/mL AmB, pH adjusted to 7.4 with NaOH.

Single-cell cytosolic Ca^{2+} measurements

Changes in $[Ca^{2+}]_i$ were monitored using the Fura-2 technique as previously described [51]. Briefly, cells on cover slips were loaded with 2 µM Fura-2 AM for 45 min in LB at room temperature in the dark. After the incubation period, cells were washed twice with LB, and left to equilibrate for at least 20 min also in LB. The coverslip was then mounted in a perfusion chamber on an inverted microscope (Olympus IX71) and perfused with different solutions at room temperature. During the recordings using Live Acquisition 2.5 software (FEI, Germany), cells were excited alternately at 340 and 380 nm using an Oligochrome excitation system (FEI, Germany) and fluorescent images were captured at 510 nm every 1 s with an ORCA-03G digital CCD camera (Hamamatsu, Germany). In our Ca^{2+} experiment results, we report the quantity

$$\mathrm{Ratio}(F_{340}/F_{380}) = \frac{F_{340,\,\mathrm{cell}} - F_{340,\,\mathrm{background}}}{F_{380,\,\mathrm{cell}} - F_{380,\,\mathrm{background}}}$$

abbreviated as R in the bar graphs, where the "background" mean fluorescence values are calculated from a region-of-interest (ROI) in each channel image (340 and 380 nm) drawn in an area without any cells.

Electron microscopy

EA.hy926 cells were grown on an Aclar film substrate (Gröpl, Tulln, Austria). The primary fixative solution contained 2.5% glutaraldehyde and 2% paraformaldehyde (Ted Pella, Redding, CA, USA) in 0.1 M phosphate buffer, pH 7.4, for 45 min.

In the process of secondary fixation, the cell sets were fixed with either 2% OsO_4 or 1% OsO_4 + 1% $K_3Fe(CN)_6$ for 45 min at room temperature. The samples were then dehydrated in increasing concentrations of acetone (25, 50, 70, 80, 90, and 95%) and in the final process of dehydration, the samples underwent three washes in 100% acetone. The cells were then resin-infiltrated in increasing concentrations of TAAB resin (30, 50, and 70% in acetone). The infiltration process was completed by three passages in 100% resin. The cells were finally resin-embedded in molds and polymerized at 60°C for 3 days.

To produce the imaging samples, 80-nm sections were cut from the embedded sample blocks with a UC 7 Ultramicrotome (Leica Microsystems, Vienna, Austria) using a diamond knife (Diatome, Biel, Switzerland) and were collected on Pioloform-coated 100-, 200-, and 300-mesh copper grids (hexagonal or square meshes; Gröpl, Tulln, Austria). The sections were post-stained with Pt-blue and Reynolds lead citrate for 15 and 7 min, respectively.

Electron micrographs at various magnifications were obtained with a Tecnai G 2 FEI transmission electron microscope at 120 kV and equipped with an ultrascan 1000cd camera (Gatan).

Cells were imaged both in a "plan" view, i.e., looking down perpendicular to the plane of the substrate on which the cells were grown, and in an "elevated" orientation, that is, observing the cells along a direction parallel to the plane of their substrate. This was done in an effort to capture as many instances of PM-ER junctions as possible and get around the difficulty of sectioning the PM effectively in the plan view due to the flatness and thinness of the cells especially at their periphery. Elevation-view blocks were prepared by cutting out a portion of a plan-view block and re-embedding it in resin tilted through 90° with respect to its original orientation.

Data analysis, statistics, software

Individual Ca^{2+} experiments in each reported set of n consist of Fura-2 signal trace measurements from approximately 5 to 20 cells. Means, standard deviations (SD), and standard errors (SEM) are then calculated for each experiment. After a set of experiments, the pooled statistics are, in turn, calculated. The reported traces and bar charts are the values of the means ± pooled SEM. In our statistical

analysis, significance was determined by Student's *t* tests; *p* values ≤0.05 were considered significant.

In reporting the PM-ER junctional parameters of membrane separation and lateral extension measured in the set of electron micrographs, we used their means ± SD to convey the spread of the recorded values.

Given the slightly different behavior observed in different sub-populations of cells, our approach to determining significance in the effects recorded under the stimuli and inhibitors used in our experiments was to analyze the ratio between the amplitudes of the Ca^{2+} transients generated by the various conditions as a measure of ER Ca^{2+} content and refilling efficiency and of cytosolic [Ca^{2+}] changes. Therefore, after calculating the mean Ca^{2+} signal traces from each type of experiment and referring to the protocol description in "ER Ca^{2+} is refilled by extracellular Ca^{2+} regardless of membrane polarization," we report our data as the amplitude ratios of the 2nd histamine transient to the 1st and of the nCa^{2+} phase transient to the 2nd histamine one. A third interesting parameter for our analysis is the rate of Ca^{2+} re-entry in the cytosol during the nCa^{2+} phase. This is calculated as the slope of the roughly linear portion of the Fura-2 signal at the onset of the nCa^{2+} phase.

The Fura-2 340/380 fluorescence ratios were recorded as text files and then analyzed by a combination of in-house C programs, Linux shell scripts and LibreOffice Calc Spreadsheet functions (http://www.libreoffice.org).

The electron micrographs were recorded as TIFF image files and analyzed with xfig (http://www.xfig.org) to measure PM-ER junctional separations and extensions, as well as "pillar" features. Plots were generated with gnuplot (http://gnuplot.info).

Results

Present knowledge suggests that the essential Ca^{2+} handling machinery at work in EC comprises TRPC and Orai1 channels, NCX and the PM Ca^{2+} ATPase (PMCA) on the PM, SERCA, and IP_3R on the ER. Indirectly involved with Ca^{2+} handling are the NKA pumps on the PM [35]. The schematic diagram in Fig. 1 provides a picture of how these players might be implicated in the shaping of Ca^{2+} signals in EC. Starting from the hypothesis that Ca^{2+} entry via the NCX is responsible at least in part for ER Ca^{2+} refilling and that this NCX-mediated refilling takes place via PM-ER junctions, we elucidated the role of the NCX by systematically inhibiting or eliminating all other potential sources of Ca^{2+} entry in EC by the employment of pharmacological agents and gene transfer techniques, in a manner that would also highlight the possible involvement of junctional transport.

ER Ca^{2+} is refilled by extracellular Ca^{2+} regardless of membrane polarization

Our main experimental protocol and basic results are displayed in Fig. 2b. The cells were kept under normal physiological conditions for the first min, then superfused with nominally Ca^{2+} free ($0Ca^{2+}$) buffer for 3 min, after which they were bathed for a further 3 min in $0Ca^{2+}$ buffer with 100 μM histamine to initiate ER Ca^{2+} release—by increasing IP_3 production and, in turn, sensitizing IP_3R to Ca^{2+}—noticeable as a Ca^{2+} transient during this phase of the protocol (the $0Ca^{2+}$ buffer choice ensures that the observed transient at this stage is solely due to Ca^{2+} mobilization from intracellular Ca^{2+} stores). Histamine is then eliminated by a 3-min washout with $0Ca^{2+}$ buffer, before superfusing cells with normal Ca^{2+} (nCa^{2+}) buffer for 4 min again to allow extracellular Ca^{2+} influx after ER Ca^{2+} release. Upon completion of the Ca^{2+} influx phase, the cells are returned to $0Ca^{2+}$ buffer before administering a second 3-min histamine stimulus aimed at revealing the amount of ER refilling that took place during the nCa^{2+} phase of the protocol. Clearly, the extracellular Ca^{2+} influx taking place during this phase manifests itself in a global $[Ca^{2+}]_i$ rise (central transient in Fig. 2b) and is able to refill the ER of the majority of its original content, as revealed by the second ER Ca^{2+} release amounting to about 67% of the first (Fig. 2b and d).

Since one of the hypotheses of the study is to understand the role of the Ca^{2+} influx mode of the NCX in the ER Ca^{2+} refilling mechanism, in all of our subsequent experiments, from 2 min prior to the nCa^{2+} phase onwards, we superfused the cells in 70 mM [K^+] buffer to depolarize the cell membrane, as a way to minimize Ca^{2+} entry via TRPC and SOCE via the STIM-Orai1 system, and thereby emphasizing the contribution of the NCX. This situation is depicted in Fig. 2a.

Moreover, depolarizing the membrane essentially clamps its potential at a value around 0 mV [41], which holds fixed the driving force of the NCX, given by the relationship $E_{NCX} < V_m$ between the NCX reversal potential, E_{NCX}, and the membrane potential, V_m. This is important since the V_m of EC (EA.hy926 included) has been shown to be rather variable [17, 22, 41] and this variability will also reflect in the driving force of the NCX. Under these experimental conditions, we recorded a greatly diminished global $[Ca^{2+}]_i$ signal during the nCa^{2+} phase, while the ER is refilled to the same level observed in cells with resting V_m (solid blue circles in Fig. 2c, d).

In this set of experiments, we also determined the contribution of extracellular Ca^{2+} as a source of ER Ca^{2+} refilling by omitting the nCa^{2+} phase from our main protocol; we

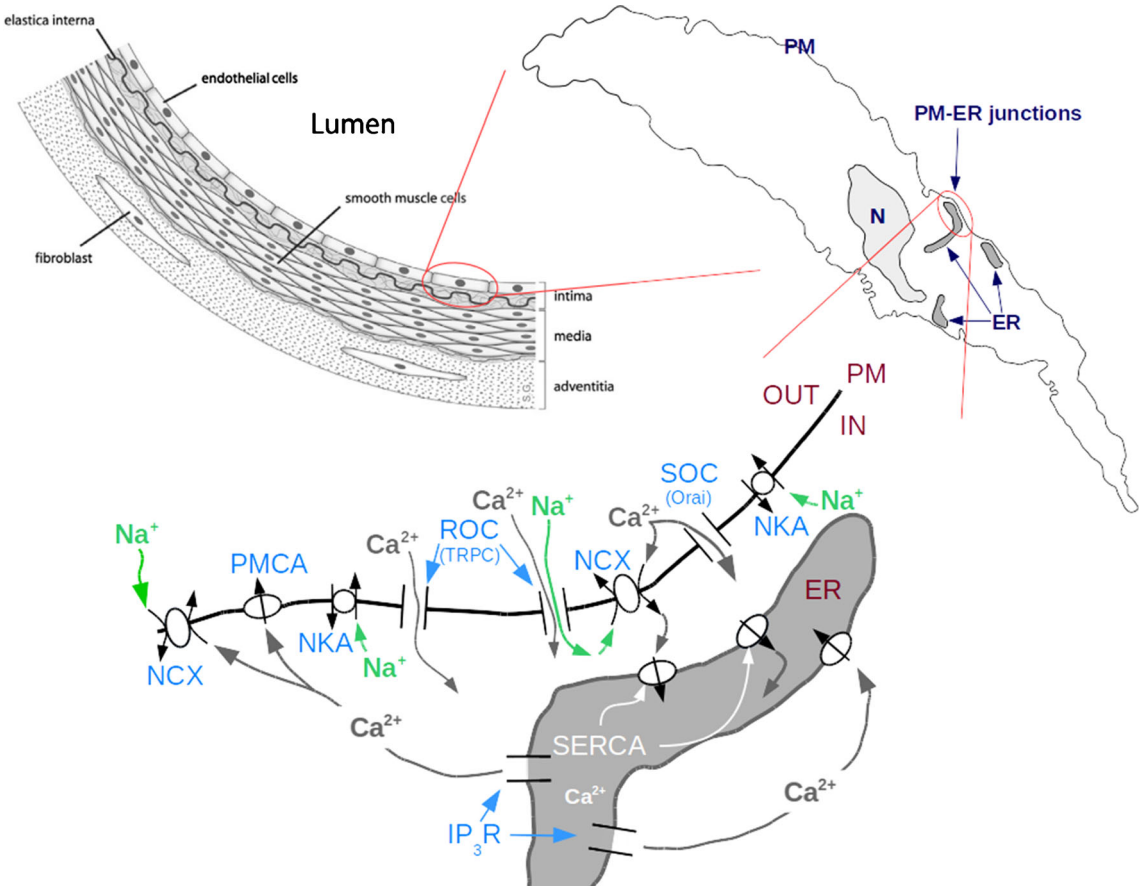

Fig. 1 *Top left*: schematic partial cross-section of a vessel with location of EC (image attribution: DRosenbach at English Wikipedia); *top right*: diagram of one EC showing location of PM-ER junctions; *bottom*: essential depiction of the current understanding of the Ca^{2+} transport machinery, ionic fluxes and some of the mechanisms responsible for ER Ca^{2+} refilling in EC. (N = nucleus; ROC = receptor operated channels; SOC = store operated channels; see text for explanations of the other acronyms)

report these data in red in Fig. 2c, d. Evidently, when external Ca^{2+} is virtually absent, there is no noticeable Ca^{2+} (re-)entry in the cytoplasm and the ER Ca^{2+} release peak is significantly lower than when extracellular Ca^{2+} is present in the superfusate. We also observed that the remnant ER Ca^{2+} in this case is largely due to re-uptake by SERCA pumps during the first ER Ca^{2+} release, since, by blocking SERCA with 2,5-Di-tert-butyl-1,4-benzoquinone (BHQ) during the first histamine stimulation, we found that the Ca^{2+} left after the second stimulation under $0Ca^{2+}$ conditions throughout the protocol was even further reduced (see section S2 in the online supplement).

NCX contribution to ER Ca^{2+} refilling

To examine whether and to what extent the NCX-mediated Ca^{2+} influx plays a role in ER refilling, we inhibited the NCX Ca^{2+} influx mode by adding 10 μM of KB-R7943 to the superfusing solution in conjunction with the cell depolarization phase of our protocol (Fig. 3; in this and the following two figures the traces obtained in the depolarization-only experiments described in the previous section—solid blue circles—are reported as reference).

Ca^{2+} release following the nCa^{2+} phase of the protocol shows that the ER Ca^{2+} refilling is about 40% less than in the reference case without KB-R7943 administration (Fig. 3b, c left). Moreover, while the relation between the Ca^{2+} re-entry and 2nd ER Ca^{2+} release transient amplitudes is comparable to the same phase in the reference data (Fig. 3c right), the average rate of re-entry during the initial nCa^{2+} phase is markedly different in the two cases (Fig. 3d).

Administering KB-R7943 after membrane depolarization ensured that non-specific effects of KB-R7943-induced TRPC channel inhibition are kept in check, since Ca^{2+} entry through those channels is already suppressed by the depolarized conditions used in our experiments.

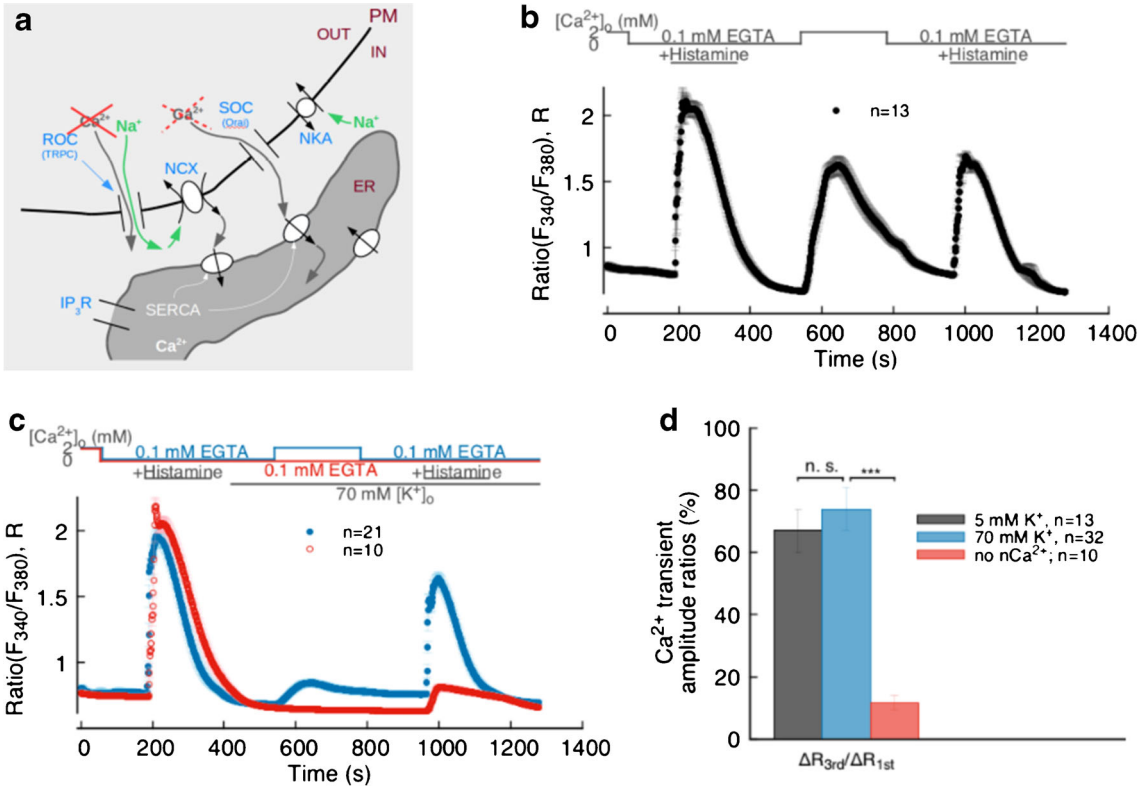

Fig. 2 **a** Schematics of the possible ion fluxes at PM-ER junctions between the extra-cellular space and ER under 70-mM-$[K^+]_o$ depolarizing condition. **b** Main protocol results under normal membrane polarization conditions: $[Ca^{2+}]_o$ and histamine stimulation timeline (*top*), recorded Fura-2 signal (*bottom*). **c** Effect of depolarization on Ca^{2+} entry and ER refilling (*solid blue circles*); effect of nCa^{2+} phase omission on the Ca^{2+} signal (*open red circles*). **d** Bar chart representing the ratio between 3rd and 1st Ca^{2+} transient amplitudes from traces in **b**, **c**. *** indicates $p<0.001$

NCX-mediated ER Ca^{2+} refilling may take place via PM-ER junctions

The observations collected to this point provide strong indication that the ER Ca^{2+} refilling mechanism under membrane depolarization conditions is all but transparent to the bulk signal. If this were also an indication that the NCX-mediated refilling is assisted by PM-ER junctions, we should see differences in the Ca^{2+} signal if we somehow interfered with junctional transport.

We attempted this by administering a low concentration of ouabain (10 nM) in the superfusate during the nCa^{2+} phase of our typical protocol. Under the working hypothesis that, like for example in vascular smooth muscle, the ouabain sensitive pumps NKA$\alpha_{2/3}$, which are likely expressed in EA.hy926 [33], reside primarily in PM-ER junctions [3, 4, 21], this type of experiment should preferentially inhibit these isoforms and, as qualitatively depicted in the schematics of Fig. 4a, in a junctional environment, the increased Na^+ accumulation due to the inhibited NKAs should enhance Ca^{2+} entry via NCX, increase ER refilling, and in essence provoke the opposite effect of KB-R7943 inhibition, that is, a higher ER Ca^{2+} release signal upon 2nd histamine stimulation. Our findings in this set of experiments corroborate the expectations, in that our measured Ca^{2+} transient amplitude during the 2nd histamine-stimulated release indicates that ER Ca^{2+} refilling levels are on average 20% higher than in the experiments without inhibition (Fig. 4b and c left). In these experiments too, we found that the ratio of the nCa^{2+}-phase transient amplitude to that of the 2nd ER Ca^{2+} release did not differ appreciably from the reference data (Fig. 4c right), while the rate of entry at the onset of the nCa^{2+} phase was significantly different (Fig. 4d).

SOCE (Orai1 channels) and NCX joint and sole contributors to ER Ca^{2+} refilling

It is evident from the results reported in Fig. 3 that a substantial fraction of ER Ca^{2+} is still releasable from the ER even after inhibition of NCX Ca^{2+} entry. This is likely only due to SOCE, since under membrane depolarization conditions and in absence of cell stimulation (note that histamine washout begins 3 min before the nCa^{2+} phase), any contribution to Ca^{2+} entry by the TRPC should be negligible. Therefore, we performed a series of NCX Ca^{2+} entry mode

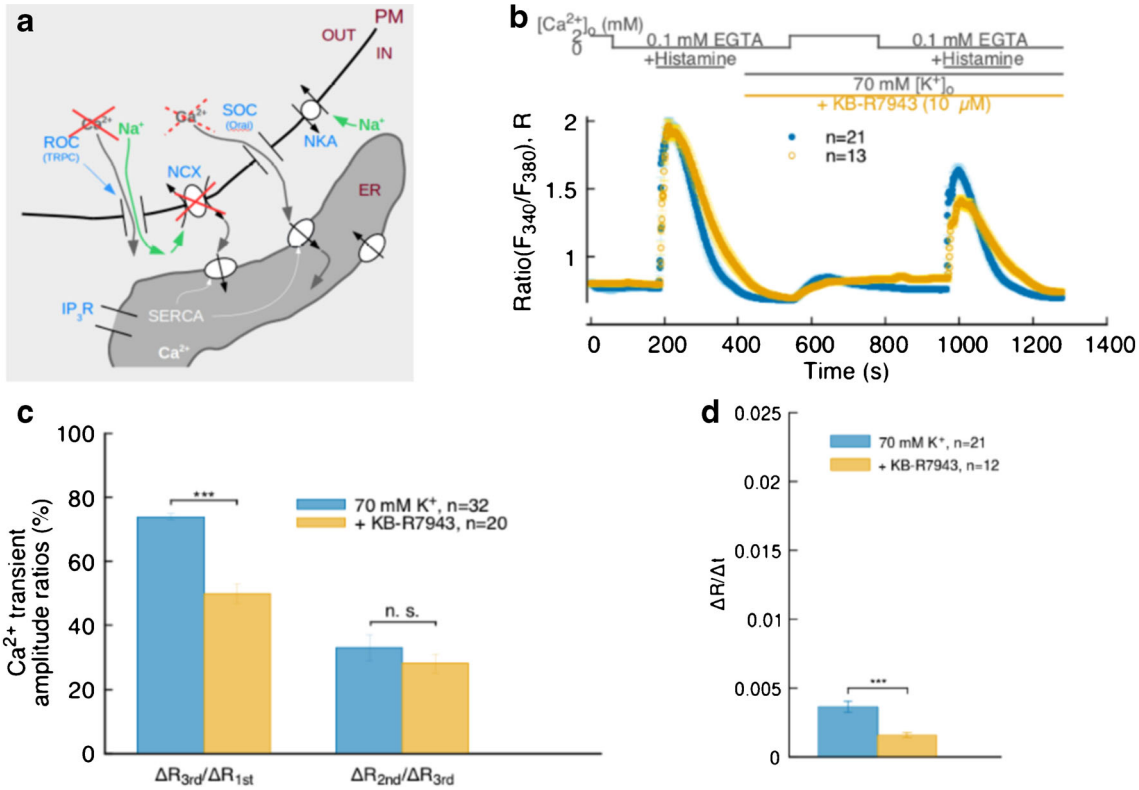

Fig. 3 **a** Schematics of the possible ion fluxes at PM-ER junction locations during the NCX Ca^{2+} influx mode inhibition experiments. **b** Effect of 10 μM KB-R7943 on ER refilling (*open yellow circles*); recordings from our standard protocol (*solid blue circles*) reported as reference. **c** Bar chart from traces in **b**; left, ratio between 3rd and 1st Ca^{2+} transient amplitudes; right, ratio between 2nd and 3rd amplitudes. **d** Bar chart from traces in B, comparing the Ca^{2+} re-entry rates into the cytoplasm at the start of the nCa^{2+} phase of the protocol. *** indicates $p<0.001$

inhibition experiments on a population of cells, which were deprived of functional Orai1 channels by means of transfection with $Orai1^{dn}$. This experimental condition should ensure inhibition and elimination of NCX and SOCE extracellular Ca^{2+} entry pathways, respectively. Results obtained with this protocol are reported in Fig. 5. The nCa^{2+} phase of the mean trace in Fig. 5b resembles closely the findings from the protocol in which the nCa^{2+} was omitted (empty red circles in Fig. 2). The amplitude ratio between the 2nd and 1st histamine transients is further attenuated compared to that of the NCX inhibition experiments (compare Figs. 5c and 3c, left). The indication from these experiments is therefore that Orai1 and NCX contribute the vast majority of the ER Ca^{2+} refilling in depolarized EC.

Ultrastructural evidence of PM-ER junctions in EA.hy926 cells

Since the collection of functional observations on Ca^{2+} handling to this point strongly suggests that the ER Ca^{2+} refilling process may be assisted by PM-ER junctions, we surveyed a set of 29 electron micrographs, like the one reported in Fig. 6a, from 12 different EA.hy926 cells, to verify that PM-ER junctions are observable in the peripheral architecture of these cells.

Image analysis revealed 41 instances of junctions with mean PM-ER separation and linear apposition extension of about 10 and 130 nm, respectively. Moreover, in at least 60% of the junctions, we observed electron opaque, somewhat irregularly spaced, junction-spanning "pillars," akin to those reported in other examples of S/ER junctions [9, 42] (Fig. 6 and Table 1). These features may in reality be present more frequently than we were able to quantify, since in a number of micrographs, although the presence of a junction is clear, the PM results too smeared to establish whether pillars are present or not (see section S3 in the online supplement).

Discussion

The results reported in this article demonstrate that in EA.hy926 EC, following IP_3R-mediated ER Ca^{2+} release, Ca^{2+} refilling occurs chiefly by Ca^{2+} entering the cytoplasm concomitantly via the NCX in Ca^{2+} entry mode and through the SOCE Orai1 channels.

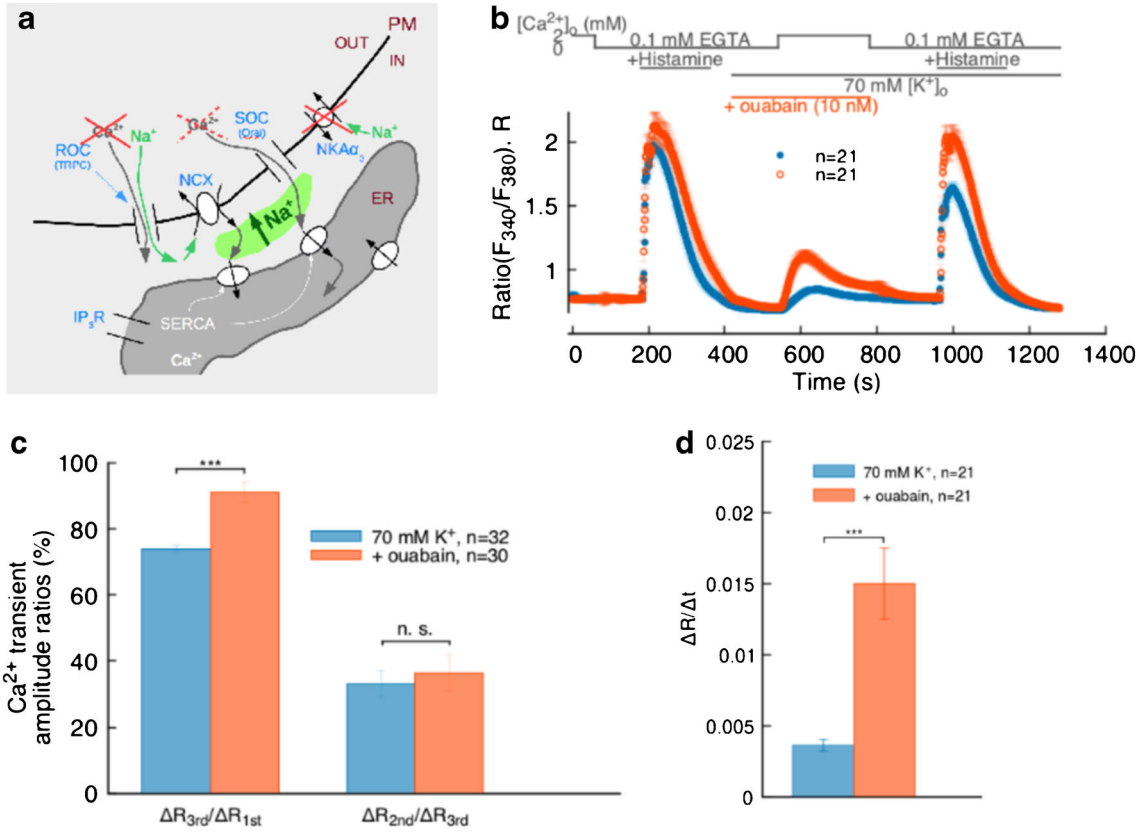

Fig. 4 **a** Schematics of the possible ion fluxes at PM-ER junctions during inhibition of ouabain sensitive NKA$\alpha_{2/3}$ pumps. **b** Effect of 10 nM ouabain on ER refilling (*open orange circles*); recordings from our standard protocol (*solid blue circles*) reported as reference. **c** Bar chart from traces in **b**; *left*, ratio between 3rd and 1st Ca^{2+} transient amplitudes; *right*, ratio between 2nd and 3rd Ca^{2+} transient amplitudes. **d** Bar chart from traces in **b**, comparing the Ca^{2+} re-entry rates at the start of the nCa^{2+} phase of the protocol. *** indicates $p<0.001$

Importantly, our findings also provide a clear indication that the refilling process taking Ca^{2+} from the extracellular space to the ER may take place via PM-ER junctions with the NCX and Orai1 sharing the transport duties almost equally. In line with this concept of junctional ER refilling, earlier work done under slightly different conditions suggested an ER refilling mechanism in this cell type acting in a manner that was undetectable in the bulk Fura-2 signal [30]. The specific Ca^{2+} transport players were not identified at that time, other than suggesting ER refilling was due to SOCE.

Using an external buffer containing 70 mM K^+ in our experimental protocols, we reduced the electrochemical gradient to a level expected to eliminate Ca^{2+} entry via the non-selective TRPC channels. These conditions ensure

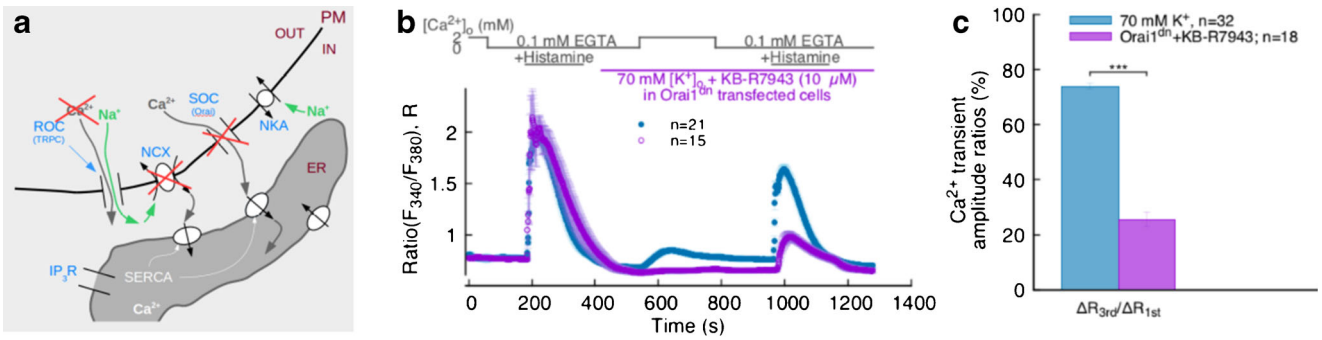

Fig. 5 **a** Schematics of the possible ion fluxes in PM-ER junctional regions during NCX inhibition in Orai1^{dn}-transfected cells. **b** Effect of 10 μM KB-R7943 on ER refilling in absence of SOCE contribution by the STIM-Orai1 system (*open purple circles*); recordings from our standard protocol (*solid blue circles*) reported as reference. **c** Bar chart representing the ratio between 3rd and 1st Ca^{2+} transient amplitudes from traces in **b**. *** indicates $p<0.001$

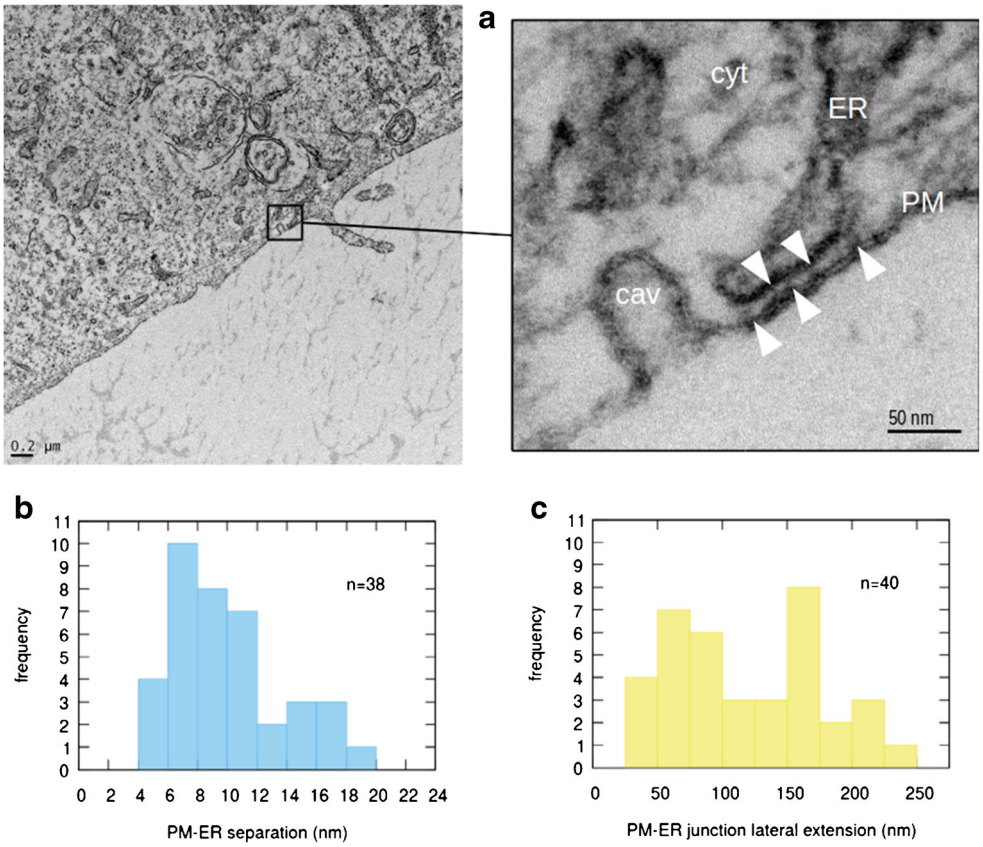

Fig. 6 **a** Representative electron micrograph of a peripheral region of an EA.hy926 cultured EC; the *right side panel* is a higher resolution image of part of the same region showing a PM-ER junction near a caveola and several instances of junction-spanning electron opaque structures (*white arrowheads*; cyt = cytoplasm, cav = caveola). **b**, **c** Histograms showing the distributions of PM-ER widths and lateral extensions, respectively

that the experiments can single out the contributions of the NCX and Orai1 to Ca^{2+} entry during the nCa^{2+} phase. A comparison between data from experiments under high K^+ conditions (Fig. 2c solid blue circles, and d) and those obtained with a physiological superfusate containing 5 mM K^+ (Fig. 2b solid black circles, and d) strongly suggests that the ER refilling mechanism is still fully functional, even after Ca^{2+} entry pathways related to TRPC and similar non-selective cation channels are suppressed. This is revealed by the not significantly different magnitude of the 2nd ER Ca^{2+} release transient amplitude between the non-depolarizing and depolarizing protocols (black and blue bars in Fig. 2d). Furthermore, since the Fura-2 signals we report are a global measure of $[Ca^{2+}]_i$ in the cell, these results indicate that the refilling must take place in a manner that all but by-passes the bulk cytosol. One way for this to occur is via PM-ER nanojunctions, in which, due to their sheer dimensions, Ca^{2+} transients are undetectable by any currently available Ca^{2+} imaging technique.

Following our process of elimination of possible sources of ER Ca^{2+} refilling, in another set of experiments, we inhibited the Ca^{2+} influx mode of the NCX with a low dose of KB-R7943 (10 µM [20]), still under depolarizing conditions. The most prominent feature of the observed signal is a markedly reduced amplitude of the 2nd ER Ca^{2+} release transient (Fig. 3b, c left) showing that inhibiting Ca^{2+} entry via NCX removes a Ca^{2+} source which contributes about 40% of the ER releasable Ca^{2+} content. Moreover, we notice no significant difference between the amplitude ratios of the nCa^{2+} phase to the 2nd ER release transients in the experiments with and without NCX inhibition (Fig. 3c right), but a significant difference between the rates of Ca^{2+} entry at the beginning of the nCa^{2+} phase of the protocol (Fig. 3d). Therefore, while substantial for the refilling of the ER, the effect of NCX inhibition on the bulk cytosolic signal is merely to slow down cytosolic Ca^{2+} re-entry without much altering the ratio between the accumulation in the bulk and that in the ER.

Table 1 Results and statistics from ultrastructural image analysis

	PM-ER separation (nm)	PM-ER linear lateral extension (nm)	Pillar thickness (nm)	Pillar separation (nm)
mean ± sd or observed range	9.6 ± 3.8	128 ± 63	4.8 ± 1.3	9–58

To further characterize the role of the NCX, we created a condition to amplify its Ca^{2+} influx mode by blocking the ouabain-sensitive NKA$\alpha_{2/3}$ pumps with 10 nM ouabain (the expression of NKAα_3 has been reported in human umbilical vein EC alongside that of the low affinity NKAα_1 [33]). If, like in vascular smooth muscle, these isoforms were primarily distributed in the PM-ER junctional regions of vascular EC [3, 4, 21], this choice would cause a strong Na^+ transient in the junctions provoking, in turn, an increased Ca^{2+} entry through the NCX and into the ER (Fig. 4a). This is indeed what we observed as reported in Fig. 4(b, c left), that is, a significantly larger amplitude ratio between the 2nd and 1st histamine-stimulated ER Ca^{2+} release transients. However, also in this experimental situation, we find that the relationship of the nCa^{2+} phase transient to the ER Ca^{2+} releasable fraction is not significantly different from the one observed in the control set (Fig. 4c right), while the rate of Ca^{2+} entry during the nCa^{2+} phase is significantly steeper (Fig. 4d). Previously, subplasmalemmal Na^+ accumulations were also reported in conjunction with the observation of histamine-induced Ca^{2+} oscillations in EC [39]. It is tempting to hypothesize that such peripherally localized Na^+ transients, a situation akin to the one we may have created in our ouabain experiments and to another observed in vascular smooth muscle cells [44], may be occurring in EC with resting V_m, as a necessary precursor to Ca^{2+} influx and consequent ER Ca^{2+} refilling mediated by NCX reversal.

Taken together, the findings from the NCX Ca^{2+} influx mode inhibition and amplification experiments are consistent with a picture suggesting that the extracellular Ca^{2+} entering through the NCX is for the most part directly sequestered in the ER, with perhaps a minor amount contributing to the cytosolic $[Ca^{2+}]$. Moreover, the ouabain-sensitive-NKA inhibition experiments also support the conjecture that the NCX Ca^{2+} transport takes place at PM-ER junctions. In this view, the fraction of bulk $[Ca^{2+}]_i$ contributed by the NCX appears marginal and due to spill-over from the junctions, which would agree with the observed decreased or increased Ca^{2+} re-entry rate upon NCX Ca^{2+} entry mode inhibition or amplification, respectively. In the former case, diminished spill-over would hinder Ca^{2+} accumulation rate in the bulk signal, in the latter, somewhat "over-driving" NCX-dependent Ca^{2+} influx would also increase Ca^{2+} escape from the junctions, which can manifest itself as a higher rate of entry in the cytosolic signal during the initial nCa^{2+} phase of the protocol.

When we inhibited NCX Ca^{2+} entry in a population of cells transfected with Orai1^{dn}, we clearly observed that SOCE via Orai1 channels contributes almost all of the releasable fraction of ER Ca^{2+} remaining after NCX inhibition in wild type cells. This can be seen in Fig. 5c, where the ratio between the 2nd and 1st histamine-stimulated transient amplitudes is further reduced to about 30% of the control experiments in (depolarized) wild type cells. Since Orai1 Ca^{2+} transport is "by definition" junctional, Orai1 SOCE must contribute to the bulk $[Ca^{2+}]_i$ via spill-over from PM-ER junctions, besides partially refilling ER Ca^{2+}.

These experiments also indicate that in virtual absence of non-selective cation channels (e.g., TRPC) contribution to the $[Ca^{2+}]_i$ signal, Orai1 channels are responsible for the near totality of the Ca^{2+} re-entry signal, which can be inferred from the complete elimination of the nCa^{2+}-phase signal in Orai1^{dn} experiments (Fig. 5b). Of note, the significant contribution of Orai1-mediated Ca^{2+} entry to junctional ER-refilling occurs even in depolarized cells with strongly reduced driving force for Ca^{2+} entry. Thus, the privileged refilling of the ER within junctional areas is likely to require minute Ca^{2+} fluxes through the highly selective Orai1 channels. That TRPC channels contribute the remainder of the bulk signal observed during the nCa^{2+} phase and virtually none of the ER Ca^{2+} releasable fraction was confirmed by NCX Ca^{2+} influx mode inhibition experiments using cells under normal V_m values (see section S4 in the online supplement).

Analyzing the dependence of the NCX reversal potential, E_{NCX}, on $[Ca^{2+}]_i$ and $[Na^+]_i$ lets us infer that the ER refilling mechanism may be assisted by PM-ER junctions also in non-depolarized cells. In Fig. 7, we plotted $E_{NCX} = 3\,E_{Na} - 2\,E_{Ca}$, where E_{Na} and E_{Ca} are the Nernst potentials for Na^+ and Ca^{2+}, respectively, as a function of $[Ca^{2+}]_i$ at 3 different possible values of $[Na^+]_i$. Two values of the membrane potential of our cells are also plotted: $V_m \approx -2$ mV (dashed blue line) is the one we expect in depolarized conditions (as we determined in [41]), while $V_m \approx -50$ mV (solid green line) is the one calculated by Goldman's equation, using permeability values found in the literature [46]. (Other reported V_m measurements in EC in the literature under physiological conditions indicate values

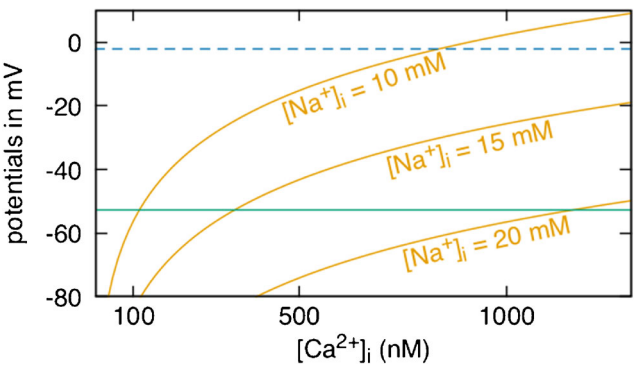

Fig. 7 NCX reversal potential *vs* $[Ca^{2+}]_i$, V_m under depolarization (70 mM K^+) conditions as measured in [41] (*blue line*) and calculated by the Goldman's equation (*green*)

virtually always around, or less negative than, −40 mV [6, 17, 22, 25, 36, 52, 55].)

Since the NCX is in Ca^{2+} influx mode when $E_{NCX} < V_m$, it is evident from the plots in Fig. 7 that in our experimental depolarizing condition of 70 mM K^+ (and $[Na^+]_o$ = 73 mM) and using typical bulk ionic concentrations values of $[Na^+]_i$ = 10 mM and $[Ca^{2+}]_o$ = 2 mM, the NCX can be expected always to function in Ca^{2+} entry mode at bulk $[Ca^{2+}]_i$ = 100 nM (the curve corresponding to E_{NCX} calculated with $[Na^+]_i$ = 10 mM is well below the depolarized V_m at $[Ca^{2+}]_i$ = 100 nM).

On the other hand, under physiological conditions of bulk cytoplasmic and of extracellular ionic concentrations normally observed in EC environment, the V_m being much more negative implies that the NCX reversal condition is barely respected at bulk $[Ca^{2+}]_i$ = 100 nM and $[Na^+]_i$ = 10 mM (the $[Na^+]_i$ = 10 mM curve crosses the $V_m \approx -50$ mV line in the neighborhood of $[Ca^{2+}]_i$ = 100 nM). As the plots suggest, assuming that $[Ca^{2+}]_i$ equals its bulk value of 100 nm, the condition would be more safely obeyed at higher values of $[Na^+]_i$ (see for example the curve corresponding to E_{NCX} calculated with $[Na^+]_i$ = 15 mM). However, according to presently available data, we can expect to observe such high Na^+ transients only in subplasmalemmal regions of cells, which are hypothesized to correspond to S/ER junctions [12, 44]. But $[Ca^{2+}]_i$ in such junctions is highly variable due to their sheer dimension and can easily reach micro-molar values [11]. In this case, the plot in Fig. 7 indicates that values of $[Na^+]_i$ closer to 20 mM would be necessary to achieve NCX reversal, which further confirms the conjecture arrived at by our functional measurements, in the depolarized system, that the NCX-mediated ER Ca^{2+} refilling mechanism must occur via PM-ER junctions in non-depolarized EC as well. (While a useful guideline, it is to a certain extent deceiving to plot continuous curves to represent the variation of E_{NCX} as a function of $[Ca^{2+}]_i$ since the latter is not known to vary continuously within the cytosol. Rather, we expect $[Ca^{2+}]_i \sim$ 100 nM and stable in the bulk cytosol, but ∼1–10 μM and highly variable in junctional environments.)

The strong indication from our Fura-2 measurements, as well as from our analysis of the electrochemical potential, that ER Ca^{2+} refilling may occur via PM-ER junctions in a privileged manner partly segregated from bulk cytosolic Ca^{2+} prompted us to study the ultrastructure of EA.hy926 cells in search for occurrences of such junctions. A survey of 29 electron micrographs suggests that peripheral ER appositions to the PM occur regularly in these cells and possess features also observed in S/ER junctions of other cells systems, which are involved in privileged Ca^{2+} signaling, such as the cardiac dyads [15], the mitochondria-ER junctions (also known as mitochondrial associated membranes (MAMs)) [8], the PM-SR junctions in vascular smooth muscle [13, 43]. We found that PM-ER junctions in EA.hy926 cells are roughly 130 nm in extension and present a mean PM-to-ER separation of about 10 nm, having thereby a ratio between separation and extension of less than 1:10 (Fig. 6 and Table 1). The further observation of junction-spanning structures in the majority of the analyzed junctions suggests, as in other cases, that these approaches of the ER to the PM are likely not random juxtapositions, but rather stable, if dynamic, features possibly able to fulfill specified functions, like the hypothesized privileged ER Ca^{2+} refilling. The architectural features of the PM-ER junctions we report herein would enable them to provide the tightly confined environment necessary to generate spatially and temporally localized high $[Ca^{2+}]_i$ and $[Na^+]_i$ transients putatively responsible for Ca^{2+} signal segregation leading to the focal ER refilling we infer from our data. Confirmation of this hypothesized role of the PM-ER junctions in EC will only be possible by a combination of specific labeling of the NCX1, Orai1, and TRPC and realistic quantitative modeling of the junctional transport dynamics.

In conclusion, our findings based on previously unavailable specific Ca^{2+} signal measurements and ultrastructural observations in the human umbilical vein-derived cell line EA.hy926 elucidate important steps in the mechanism of ER Ca^{2+} refilling and indicate that most of the ER Ca^{2+} releasable fraction is transported from the extra-cellular space to the ER lumen by the NCX and the Orai1 channels in similar proportions. In light of a hypothesized link between Na^+/Ca^{2+} exchange-mediated Ca^{2+} entry and eNOS activation which had been observed upon Na^+ loading in ECs [49], our contribution is likely a useful step forward in understanding important features of the overall EC function of NO production via eNOS. Furthermore, the transport appears to take place via PM-ER junctions, which we identified and characterized for the first time. Our data therefore suggest that PM-ER junctions in EC can constitute an active functional unit for directed Ca^{2+} transport much like the hypothesized "subplasmalemmal Ca^{2+} control unit (SCCU)" [16] and the superficial buffer barrier [53].

Acknowledgements We acknowledge the feedback and input from Gerd Leitinger, and the invaluable technical support of Elizabeth Pritz, Michaela Janschitz, René Rost, and Anna Schreilechner. We express our gratitude to C. J. Edgell, Pathology Department, University of North Carolina at Chapel Hill, NC, USA, for providing the EA.hy926 cells and generating the initial population.

This project has received funding from the European Union's Seventh Framework Programme for research, technological development and demonstration under grant agreement no. PIIF-GA-2012-330657 to Nicola Fameli and Klaus Groschner (QuMoCa project; qumoca.org), from the Austrian Science Fund (FWF) grant no. W1226 to Klaus Groschner, and from the Canadian Institute of Health Research under grant no. CIHR MOP-84309 to Cornelis van Breemen. Open access funding provided by the Medical University of Graz.

References

1. Andrikopoulos P, Baba A, Matsuda T, Djamgoz MBA, Yaqoob MM, Eccles SA (2011) Ca2+ influx through reverse mode na+/ca2+ exchange is critical for vascular endothelial growth factor-mediated extracellular signal-regulated kinase (erk) 1/2 activation and angiogenic functions of human endothelial cells. J Biol Chem 286(44):37919–37931
2. Antigny F, Jousset H, Kònig S, Frieden M (2011) Thapsigargin activates ca^2+ entry both by store-dependent, stim1/orai1-mediated, and store-independent, trpc3/plc/pkc-mediated pathways in human endothelial cells. Cell Calcium 49(2):115–127
3. Arnon A, Hamlyn JM, Blaustein MP (2000) Ouabain augments ca(2+) transients in arterial smooth muscle without raising cytosolic na(+). Am J Physiol Heart Circ Physiol 279(2):H679–H691
4. Blaustein MP, Zhang J, Chen L, Song H, Raina H, Kinsey SP, Izuka M, Iwamoto T, Kotlikoff MI, Lingrel JB, Philipson KD, Wier WG, Hamlyn JM (2009) The pump, the exchanger, and endogenous ouabain: signaling mechanisms that link salt retention to hypertension. Hypertension 53(2):291–298
5. Bondarenko AI, Drachuk K, Panasiuk O, Sagach V, Deak AT, Malli R, Graier WF (2013) N-arachidonoyl glycine suppresses na/ca^2 exchanger-mediated ca^2 entry into endothelial cells and activates bk(ca) channels independently of gpcrs. Br J Pharmacol 169(4):933–948
6. Bregestovski P, Bakhramov A, Danilov S, Moldobaeva A, Takeda K (1988) Histamine-induced inward currents in cultured endothelial cells from human umbilical vein. Br J Pharmacol 95(2):429–436
7. Cabello OA, Schilling WP (1993) Vectorial ca2+ flux from the extracellular space to the endoplasmic reticulum via a restricted cytoplasmic compartment regulates inositol 1,4,5-trisphosphate-stimulated ca2+ release from internal stores in vascular endothelial cells. Biochem J 295(Pt 2):357–366
8. Csordàs G, Renken C, Vàrnai P, Walter L, Weaver D, Buttle KF, Balla T, Mannella CA, Hajnòczky G (2006) Structural and functional features and significance of the physical linkage between er and mitochondria. J Cell Biol 174(7):915–921
9. Devine CE, Somlyo AV, Somlyo AP (1972) Sarcoplasmic reticulum and excitation-contraction coupling in mamMalian smooth muscles. J Cell Biol 52(3):690–718
10. Edgell CJ, McDonald CC, Graham JB (1983) Permanent cell line expressing human factor viii-related antigen established by hybridization. Proc Natl Acad Sci USA 80(12):3734–3737
11. Fameli N, Breemen C (2012) The role of cytoplasmic nanospaces in smooth muscle cell ca2+ signalling. Protoplasma 249(1):S39–S48
12. Fameli N, Kuo K-H, van Breemen C (2009) A model for the generation of localized transient [na+] elevations in vascular smooth muscle. Biochem Biophys Res Commun 389(3):461–465
13. Fameli N, Ogunbayo OA, van Breemen C, Evans AM (2014) Cytoplasmic nanojunctions between lysosomes and sarcoplasmic reticulum are required for specific calcium signaling. F1000Res 3:93
14. Fameli N, van Breemen C, Kuo K-H (2007) A quantitative model for linking na+/ca2+ exchanger to serca during refilling of the sarcoplasmic reticulum to sustain [ca2+] oscillations in vascular smooth muscle. Cell Calcium 42(6):565–575
15. Franzini-Armstrong C, Protasi F, Ramesh V (1999) Shape, size, and distribution of ca(2+) release units and couplons in skeletal and cardiac muscles. Biophys J 77(3):1528–1539
16. Graier WF, Paltauf-Doburzynska J, Hill BJ, Fleischhacker E, Hoebel BG, Kostner GM, Sturek M (1998) Submaximal stimulation of porcine endothelial cells causes focal ca2+ elevation beneath the cell membrane. J Physiol 506(1):109–125
17. He P, Curry FE (1995) Measurement of membrane potential of endothelial cells in single perfused microvessels. Microvasc Res 50(2):183–198
18. Himmel HM, Whorton AR, Strauss HC (1993) Intracellular calcium, currents, and stimulus-response coupling in endothelial cells. Hypertension 21(1):112–127
19. Ignarro LJ, Buga GM, Wood KS, Byrns RE, Chaudhuri G (1987) Endothelium-derived relaxing factor produced and released from artery and vein is nitric oxide. Proc Natl Acad Sci USA 84(24):9265–9269
20. Iwamoto T, Watano T, Shigekawa M (1996) A novel isothiourea derivative selectively inhibits the reverse mode of na+/ca2+ exchange in cells expressing ncx1. J Biol Chem 271(37):22391–22397
21. Juhaszova M, Blaustein MP (1997) Na+ pump low and high ouabain affinity alpha subunit isoforms are differently distributed in cells. Proc Natl Acad Sci USA 94(5):1800–1805
22. Kamouchi M, Droogmans G, Nilius B (1999) Membrane potential as a modulator of the free intracellular ca2+ concentration in agonist-activated endothelial cells. Gen Physiol Biophys 18(2):199–208
23. Kòhler R, Brakemeier S, Kùhn M, Degenhardt C, Buhr H, Pries A, Hoyer J (2001) Expression of ryanodine receptor type 3 and trp channels in endothelial cells: comparison of in situ and cultured human endothelial cells. Cardiovasc Res 51(1):160–168
24. Lagaud G, Gaudreault N, Moore EDW, Van Breemen C, Laher I (2002) Pressure-dependent myogenic constriction of cerebral arteries occurs independently of voltage-dependent activation. Am J Physiol Heart Circ Physiol 283(6):H2187–H2195
25. Laskey RE, Adams DJ, Johns A, Rubanyi GM, van Breemen C (1990) Membrane potential and na(+)-k+ pump activity modulate resting and bradykinin-stimulated changes in cytosolic free calcium in cultured endothelial cells from bovine atria. J Biol Chem 265(5):2613–2619
26. Lee C-H, Kuo K-H, Dai J, Leo JM, Seow CY, Breemen C (2005) Calyculin-a disrupts subplasmalemmal junction and recurring ca2+ waves in vascular smooth muscle. Cell Calcium 37(1):9–16
27. Lee CH, Poburko D, Sahota P, Sandhu J, Ruehlmann DO, van Breemen C (2001) The mechanism of phenylephrine-mediated [Ca(2+)](i) oscillations underlying tonic contraction in the rabbit inferior vena cava. J Physiol 534(Pt 3):641–650
28. Lesh RE, Marks AR, Somlyo AV, Fleischer S, Somlyo AP (1993) Anti-ryanodine receptor antibody binding sites in vascular and endocardial endothelium. Circ Res 72(2):481–488
29. Liang W, Buluc M, van Breemen C, Wang X (2004) Vectorial ca2+ release via ryanodine receptors contributes to ca2+ extrusion from freshly isolated rabbit aortic endothelial cells. Cell Calcium 36(5):431–443
30. Malli R, Frieden M, Hunkova M, Trenker M, Graier WF (2007) Ca2+ refilling of the endoplasmic reticulum is largely preserved albeit reduced ca2+ entry in endothelial cells. Cell Calcium 41(1):63–76
31. Malli R, Frieden M, Trenker M, Graier WF (2005) The role of mitochondria for ca2+ refilling of the endoplasmic reticulum. J Biol Chem 280(13):12114–12122

32. Marsen TA, Simonson MS, Dunn MJ (1996) Roles of calcium and kinases in regulation of thrombin-stimulated preproendothelin-1 transcription. Am J Physiol 271(5 Pt 2):H1918–H1925
33. Mayol V, Dignat-George F, Gerbi A, Martin-Vasallo P, Lesaule G, Sampol J, Maixent JM (1998) Evidence that human endothelial cells express different isoforms of na,k-atpase. J Hypertens 16:145–150
34. Moccia F, Berra-Romani R, Tanzi F (2012) Update on vascular endothelial ca(2+) signalling: a tale of ion channels, pumps and transporters. World J Biol Chem 3(7):127–158
35. Nakagawa M, Takamatsu H, Toyoda T, Sawada S, Tsuji H, Ijichi H (1987) Effect of inhibition of na+-k+ atpase on the prostacyclin generation of cultured human vascular endothelial cells. Life Sci 40(4):351–357
36. Northover BJ (1980) The membrane potential of vascular endothelial cells. Adv Microcirc 9:135
37. Okeke E, Dingsdale H, Parker T, Voronina S, Tepikin AV (2016) Endoplasmic reticulum-plasma membrane junctions: structure, function and dynamics. J Physiol 594(11):2837–2847
38. Palmer RM, Ferrige AG, Moncada S (1987) Nitric oxide release accounts for the biological activity of endothelium-derived relaxing factor. Nature 327(6122):524–526
39. Paltauf-Doburzynska J, Frieden M, Spitaler M, Graier WF (2000) Histamine-induced ca2+ oscillations in a human endothelial cell line depend on transmembrane ion flux, ryanodine receptors and endoplasmic reticulum ca2+-atpase. J Physiol 524(3):701–713
40. Paltauf-Doburzynska J, Posch K, Paltauf G, Graier WF (1998) Stealth ryanodine-sensitive ca2+ release contributes to activity of capacitative ca2+ entry and nitric oxide synthase in bovine endothelial cells. J Physiol 513(2):369–379
41. Pelzmann B, Di Giuro CML, Zorn-Pauly K, Rossmann C, Hallström S, Groschner K, Fameli N (2016) Functional impairment of endothelial cells by the antimycotic amphotericin b. Biochem Biophys Res Commun
42. Poburko D, Fameli N, Kuo K-H, van Breemen C (2008) Ca2+ signaling in smooth muscle: TRPC6, NCX and LNats in nanodomains. Channels (Austin Tex.) 2(1):10–12
43. Poburko D, Kuo K-H, Dai J, Lee C-H, van Breemen C (2004) Organellar junctions promote targeted ca2+ signaling in smooth muscle: why two membranes are better than one. Trends Pharmacol Sci 25(1):8–15
44. Poburko D, Liao C-H, Lemos VS, Lin E, Maruyama Y, Cole WC, van Breemen C (2007) Transient receptor potential channel 6-mediated, localized cytosolic [na+] transients drive na+/ca2+ exchanger-mediated ca2+ entry in purinergically stimulated aorta smooth muscle cells. Circ Res 101(10):1030–1038
45. Quednau BD, Nicoll DA, Philipson KD (1997) Tissue specificity and alternative splicing of the na+/ca2+ exchanger isoforms ncx1, ncx2, and ncx3 in rat. Am J Physiol 272(4 Pt 1):C1250–C1261
46. Smith QR, Rapoport SI (1986) Cerebrovascular permeability coefficients to sodium, potassium, and chloride. J Neurochem 46(6):1732–1742
47. Strait KA, Stricklett PK, Kohan JL, Miller MB, Kohan DE (2007) Calcium regulation of endothelin-1 synthesis in rat inner medullary collecting duct. Am J Physiol Renal Physiol 293(2):F601–F606
48. Szewczyk MM, Davis KA, Samson SE, Simpson F, Rangachari PK, Grover AK (2007) Ca2+-pumps and na2+-ca2+-exchangers in coronary artery endothelium versus smooth muscle. J Cell Mol Med 11(1):129–138
49. Teubl M, Groschner K, Kohlwein SD, Mayer B, Schmidt K (1999) Na(+)/ca(2+) exchange facilitates ca(2+)-dependent activation of endothelial nitric-oxide synthase. J Biol Chem 274:29529–29535
50. Tran QK, Ohashi K, Watanabe H (2000) Calcium signalling in endothelial cells. Cardiovasc Res 48(1):13–22
51. Tsien RY, Rink TJ, Poenie M (1985) Measurement of cytosolic free ca2+ in individual small cells using fluorescence microscopy with dual excitation wavelengths. Cell Calcium 6(1-2):145–157
52. Vaca L, Licea A, Possani LD (1996) Modulation of cell membrane potential in cultured vascular endothelium. Am J Physiol 270(3 Pt 1):C819–C824
53. Van Breemen C (1977) Calcium requirement for activation of intact aortic smooth muscle. J Physiol 272(2):317–329
54. van Breemen C, Fameli N, Evans AM (2013) Pan-junctional sarcoplasmic reticulum in vascular smooth muscle: nanospace ca2+ transport for site- and function-specific ca2+ signalling. J Physiol 591(8):2043–2054
55. Vargas FF, Caviedes PF, Grant DS (1994) Electrophysiological characteristics of cultured human umbilical vein endothelial cells. Microvasc Res 47(2):153–165
56. Wang X, Reznick S, Li P, Liang W, van Breemen C (2002) Ca(2+) removal mechanisms in freshly isolated rabbit aortic endothelial cells. Cell Calcium 31(6):265–277